Invited Paper

Performance of PM QPSK and PM 16-QAM coherent optical fiber communication systems

J. C. Cartledge*[a], J. D. Downie[b], J. E. Hurley[b], A. S. Karar[a], J. H. Ke[a], I. Roudas[b], and K. Roberts[c]
[a]Queen's University, Kingston, ON, Canada K7L 3N6
[b]Corning Inc., Corning, NY, USA 14831
[c]Ciena Corp., Ottawa, ON, Canada K2H 8E9

ABSTRACT

The performance of polarization multiplexed, quadrature phase shift keying (PM QPSK) and polarization multiplexed 16-ary quadrature amplitude modulation (PM 16-QAM) is considered with an emphasis on the signal processing algorithms that compensate transmission impairments and implement key receiver functions.

Keywords: Coherent optical communications, signal processing, system performance

1. INTRODUCTION

In optical fiber communications, the realization of suitable high-speed digital-to-analog converters, analog-to-digital converters, and digital signal processors has allowed advanced signal processing to offer substantial improvements in system performance and functionality. The signal processing is performed in the transmitter or the receiver. In the transmitter, appropriate drive signals for an optical modulator are synthesized using digital signal processing and digital-to-analog conversion. This permits the generation of modulated optical signals with unprecedented control of the time-varying amplitude and phase. For example, the transmitted signal can be pre-compensated to account for the dispersion of an optical fiber, fiber nonlinear effects, and the filtering of reconfigurable optical add-drop multiplexers. In the receiver, the combination of coherent detection, analog-to-digital conversion, and digital signal processing has proven to be a particularly powerful approach. Coherent detection preserves both the amplitude and phase of the received optical signal in the photodetected signal. This allows for post-compensation using digital signal processing that effectively mitigates linear transmission impairments and implements key receiver functions.

In coherent optical transmission systems, polarization multiplexed, quadrature phase shift keying[1] (PM QPSK) and polarization multiplexed, 16-ary quadrature amplitude modulation[2] (PM 16-QAM) can be used to achieve an increase in the spectral efficiency. For PM QPSK, two-level drive signals are required for the IQ optical modulator, while for PM 16-QAM, four-level drive signals are required. The four-level drive signals can be generated using either the RF combining of two two-level signals[2] or a high-speed digital signal processor and digital-to-analog converters (DACs)[3-11].

The performance of coherent optical fiber communication systems depends on the signal processing algorithms and on their implementation. Due to the high cost of developing an ASIC or FPGA based solution for receiver real-time processing at the symbol rates of interest, it is common practice in research to use a real-time sampling oscilloscope to perform the analog-to-digital conversion and off-line computer processing of the captured waveforms to perform the signal processing. In this paper, we illustrate the role of the signal processing algorithms on the transmission performance of systems using PM QPSK and PM 16-QAM signals.

2. PM QPSK EXPERIMENTAL SETUP

A simplified illustration of the experimental setup for PM QPSK is shown in Figure 1. Four DFB lasers with nominal linewidths of 5 MHz and spaced by 50 GHz were multiplexed together and modulated by an IQ modulator driven by two 2^{15}-1 PRBS patterns at 28 Gbit/s (allowing for the FEC coding overhead). The output from the IQ modulator was split and then recombined in orthogonal polarizations after delaying one of the signals to decorrelate it from the other signal.

*john.cartledge@queensu.ca; phone +1 613 533 2935

Next-Generation Optical Communication: Components, Sub-Systems, and Systems,
edited by Guifang Li, Dieter Stefan Jäger, Proc. of SPIE Vol. 8284, 82840C · © 2012 SPIE
CCC code: 0277-786X/12/$18 · doi: 10.1117/12.910847

The PM-QPSK signals were launched into a recirculating loop which had three spans with each span comprised of 100 km of a developmental ultra low-loss, large effective area fiber and 100 km of ultra low-loss single mode fiber (Corning® SMF-28® ULL). The span loss was compensated by a single stage erbium doped fiber amplifier and backward pumped distributed Raman amplifier. A loop synchronous polarization scrambler was used to mitigate possible loop polarization artifacts. The measured channel was amplified and filtered (0.4 nm bandwidth) before detection by a polarization- and phase-diverse coherent receiver that used a local oscillator laser with a nominal linewidth of 100 KHz. The four signals from the balanced photodetectors were digitized by 50 GSa/s analog-to-digital converters using a real-time sampling oscilloscope with 20 GHz electrical bandwidth.

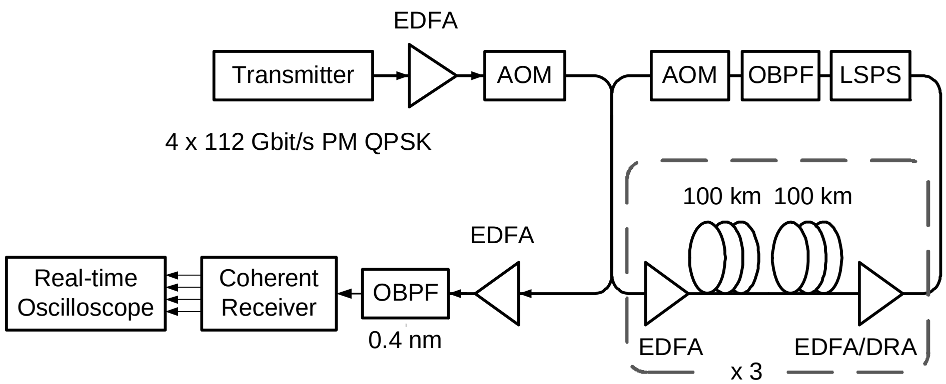

Figure 1. Experimental setup for transmission measurements. EDFA: erbium doped fiber amplifier. AOM: acousto-optic modulator. OBPF: optical bandpass filter. LSPS: loop synchronous polarization scrambler. DRA: distributed Raman amplifier.

The off-line signal processing included (i) quadrature imbalance compensation[12], (ii) re-sampling to 56 GSa/s and chromatic dispersion compensation using a fixed time- or frequency-domain equalizer, (iii) digital square and filter clock recovery[13], (iv) polarization recovery and residual dispersion compensation using 15-tap (unless indicated otherwise) adaptive equalizers in a butterfly configuration and the constant modulus algorithm[14,15], (v) carrier frequency recovery using a spectral domain algorithm[16], (vi) carrier phase recovery using the pre-decision[17], decision-directed maximum-likelihood (DD-ML)[18], 4^{th} power with zero lag smoothing (ZLS)[19], and second order phase lock loop (PLL)[20] algorithms, and (vii) symbol decisions. These algorithms involve removing the modulation from the total phase of the signal and filtering (i.e., averaging) to reduce the impact of ASE noise on the estimation of the relatively slowly varying laser phase noise. The bit error ratio (BER) was obtained by direct bit error counting. With suitable values for the parameters in the signal processing algorithms, cycle slips were not observed. Consequently, differential coding was not used.

3. PM QPSK RESULTS

The focus of this experiment was to assess the implications of the transmitted power for the developmental ultra low-loss, large effective area fiber. Figure 2 illustrates the dependence of the BER on the transmitted power for the four carrier phase estimation algorithms. The transmission distance is 2400 km. The BER performance is remarkably similar for the four algorithms. The performance is limited by the optical signal-to-noise ratio (OSNR) for small transmitted powers and by fiber nonlinearities for large powers. Figure 2 also shows the corresponding dependence of the average conditional variance of the decision samples on the transmitted power for the four carrier phase estimation algorithms. For each value of the transmitted power, the average conditional variance was obtained by averaging the variances for the eight conditional density functions (corresponding to the X and Y polarizations, in-phase and quadrature components, +1 and -1 transmitted bits). For this, the QPSK constellation was decomposed into two BPSK constellations (0 and π), or equivalently two ASK constellations (-1 and +1), for the in-phase and quadrature components. An example of the histogram for the in-phase, X-polarization signal is shown in Figure 3 for the DD-ML algorithm. The average conditional variance does not distinguish the OSNR limited results from the fiber nonlinearity limited results.

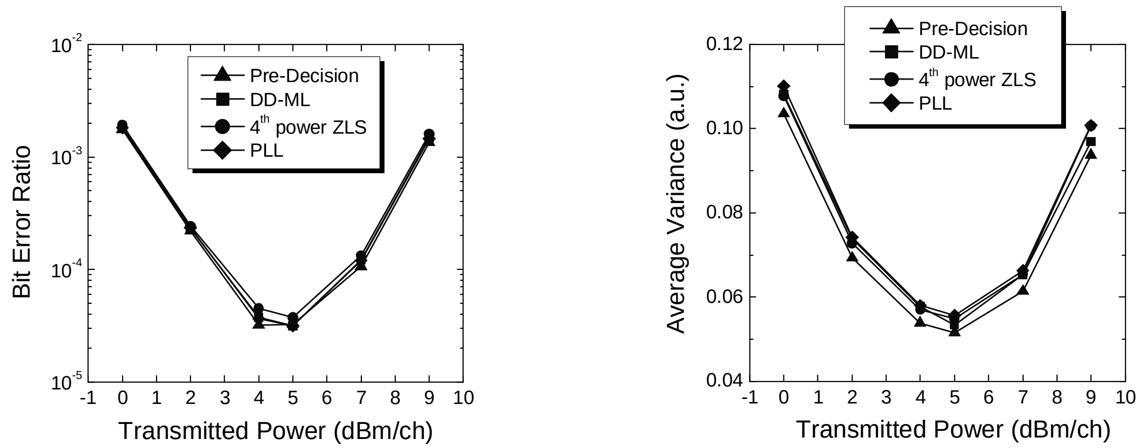

Figure 2. Left: dependence of the BER on the transmitted power per channel for four carrier phase estimation algorithms. Right: dependence of the average variance on the transmitted power per channel for four carrier phase estimation algorithms. The transmission distance is 2400 km.

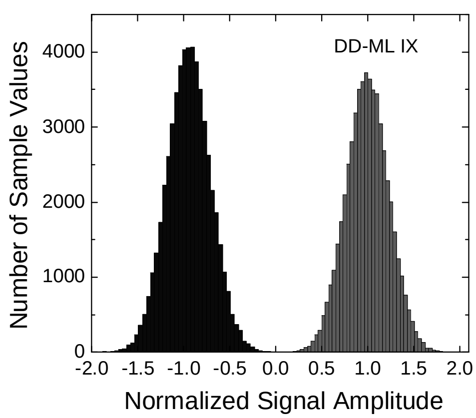

Figure 3. Histograms for the sample values for the in-phase component of the X-polarization signal. Transmitted power is 5 dBm/ch.

The dependence of the BER on the averaging (i.e., filter length) in the carrier phase estimation algorithms (with 15 taps for the adaptive equalizer) and on the number of taps for the adaptive equalizer (with a filter length of 16 for the pre-decision and DD-ML algorithms, and 33 for the 4^{th} power ZLS algorithm) is shown in Figure 4. The amount of averaging in the phase estimation algorithm can be optimized as a trade-off exists between estimating the laser phase noise accurately (small amount of averaging) and reducing the impact of amplified spontaneous emission (ASE) noise on the estimate (large amount of averaging). As the number of taps increases, the performance improves but with a diminishing improvement for more than 11 taps.

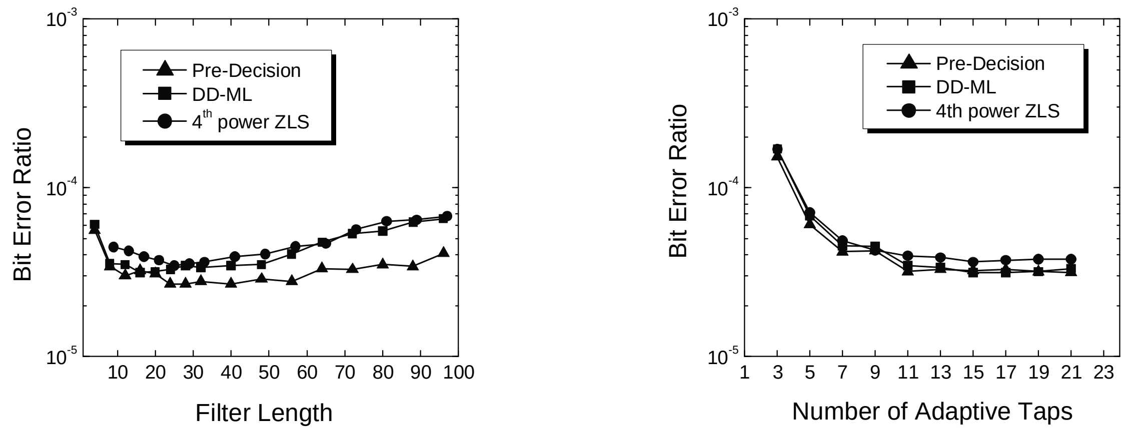

Figure 4. Left: dependence of the BER on the filter length for the pre-decision, DD-ML, and 4th power ZLS algorithms (with 15 taps for the adaptive equalizer). Right: dependence of the BER on the number of taps for the adaptive equalizer (with a filter length of 16 for the pre-decision and DD-ML algorithms, and 33 for the 4th power ZLS algorithm). The transmission distance is 2400 km.

4. PM 16-QAM EXPERIMENTAL SETUP

A simplified illustration of the experimental setup for PM 16-QAM is shown in Figure 5. Measured results were obtained for an angle differential encoded[20,21] 85.672 Gbit/s PM 16-QAM signal (allowing for the FEC coding overhead) that was generated using an external cavity laser with a nominal linewidth of 100 KHz, an ASIC with two DACs (sampling rate of 21.418 GSa/s and resolution of 6 bits), and an IQ modulator (Figure 6). A 2^{16} de Bruijn bit sequence was used for bit to symbol mapping and the generation of the in-phase and quadrature signals. The optical pulse shape at the output of the modulator had a raised-cosine spectrum with a roll-off factor of 1. The output signal from the IQ modulator was split and then recombined in orthogonal polarizations after delaying one of the signals to decorrelate it from the other signal. The PM 16-QAM signal was combined with thirty-seven 112 Gbit/s PM QPSK signals in a recirculating loop experiment. Thirty-seven DFB lasers were multiplexed together and modulated by an IQ modulator driven by two 2^{15}-1 PRBS patterns at 28 Gbit/s. The 112 Gbit/s PM QPSK signals were obtained by polarization multiplexing. The PM 16-QAM and nearest PM QPSK signals were spaced by 100 GHz; the PM QPSK signals above and below the PM 16-QAM signal were spaced by 50 GHz. The recirculating loop was comprised of three 100 km spans of Corning® Vascade® EX2000 optical fiber with a dispersion coefficient of 19.4 ps/km/nm at 1550 nm and an average attenuation of 0.162 dB/km. The fiber dispersion was post-compensated in the receiver. Raman amplification was used for each span with counter-propagating pump signals at wavelengths of 1427 nm, 1443 nm and 1462 nm. The loop included a synchronous polarization scrambler and a WaveShaper to equalize the channel powers. The average launch power was -4 dBm for each of the PM QPSK signals and -6 dBm for the PM 16-QAM signal. The PM 16-QAM signal was amplified by an EDFA and filtered (0.4 nm bandwidth) before detection by a polarization- and phase-diverse coherent receiver that used a local oscillator external cavity laser with a nominal linewidth of 100 KHz. The four signals from the balanced photodetectors were digitized by 50 GSa/s analog-to-digital converters using a real-time oscilloscope with 20 GHz electrical bandwidth.

The off-line signal processing included (i) quadrature imbalance compensation[12], (ii) re-sampling to 21.418 GSa/s and fiber dispersion compensation using fixed frequency-domain equalization, (iii) digital square and filter clock recovery[13], (iv) polarization recovery and residual distortion compensation using 11-tap (unless indicated otherwise) adaptive equalizers in a butterfly configuration, (v) carrier frequency recovery using either a spectral domain algorithm[16,22] or an 8th order algorithm[23], (vi) phase recovery using the blind phase search (BPS) algorithm[24], two stage BPS algorithm[25], or combined BPS and maximum likelihood (BPS-ML) algorithm[26], (vii) symbol decisions and (viii) angle differential decoding. The adaptive equalizer used a constant modulus algorithm for pre-convergence followed by a radius directed algorithm[27]. The BER was obtained by direct bit error counting using rectilinear decision boundaries.

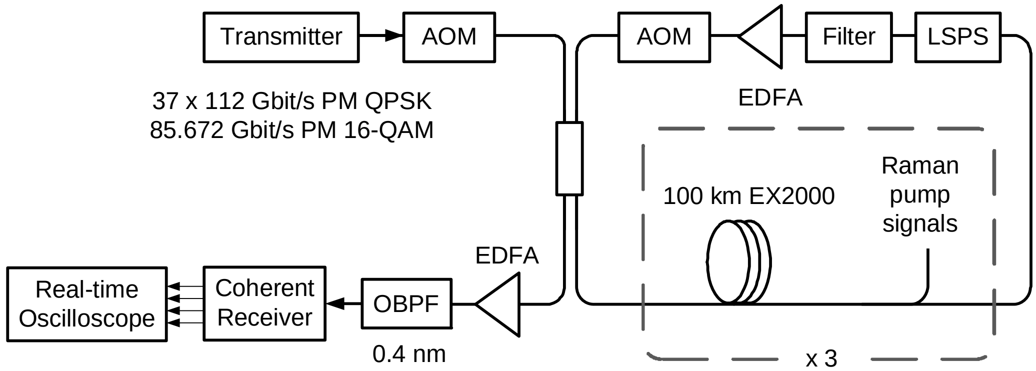

Figure 5. Experimental setup for transmission measurements. AOM: acousto-optic modulator. EDFA: erbium doped fiber amplifier. LSPS: loop synchronous polarization scrambler. VOA: variable optical attenuator. OBPF: optical bandpass filter.

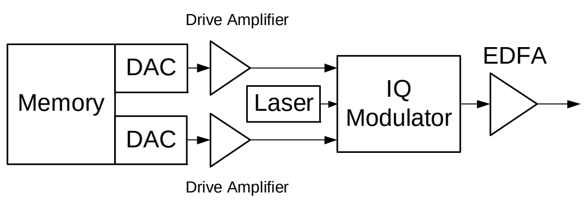

Figure 6. Transmitter for 16-QAM signal. DAC: digital-to-analog converter. IQM: IQ modulator. EDFA: erbium doped fiber amplifier.

5. PM 16-QAM RESULTS

The focus of this experiment was to assess the system reach for a PM 16-QAM signal generated with the transmitter shown in Figure 6. Figure 7 illustrates the impact of the number of taps in the adaptive equalizer on the BER performance for transmission distances of 1200 to 2400 km. As the number of taps increases from 7 to 21, the performance improves and then worsens. For the cases considered here, 11 taps provides the best performance for all fiber lengths.

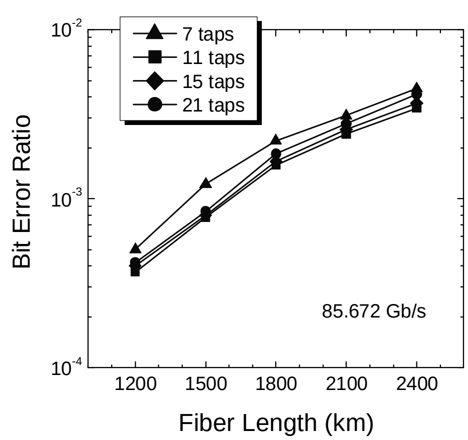

Figure 7. Dependence of the BER on the fiber length for a different number taps for the adaptive equalizer. BPS carrier phase estimation algorithm.

The dependence of the BER on fiber length is shown in Figure 8 for different values of the convergence parameter μ in the adaptation algorithm for the filter tap weights. The number of taps is 11. The performance is similar for values of 0.8×10^{-5} to 1.2×10^{-5} but worsens when the convergence parameter increases or decreases by a factor of 5 relative to the near-optimum value of 1.0×10^{-5}.

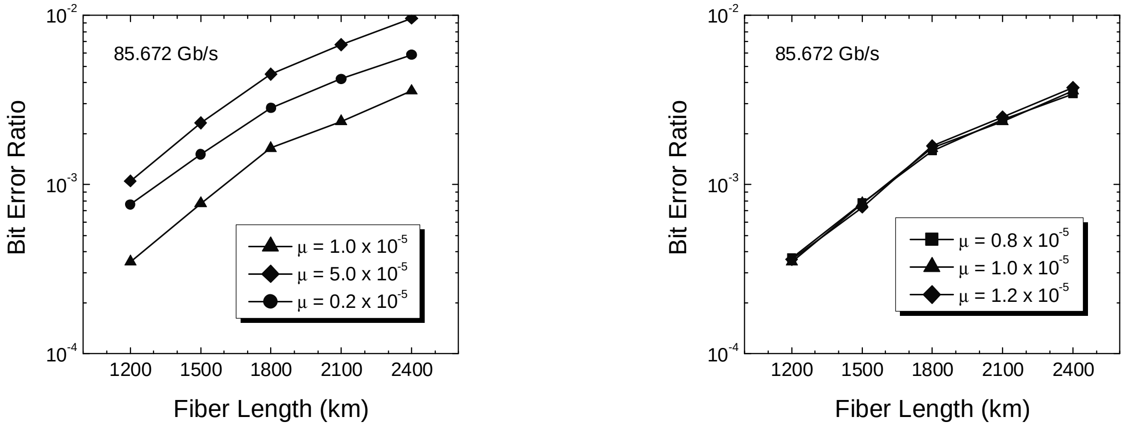

Figure 8. Dependence of the BER on fiber length for different values of the convergence parameter. 11-tap adaptive equalizer; BPS carrier phase estimation algorithm.

Figure 9 illustrates results for the dependence of the BER on fiber length for combinations of two frequency offset estimation algorithms (spectral domain and 8th order) and two carrier phase estimation algorithms (BPS and BPS-ML). In this particular case, the spectral domain frequency offset estimation algorithm yields better performance than the 8th order algorithm. This is attributed to the extent to which the assumptions made in deriving the 8th order algorithm actually hold.

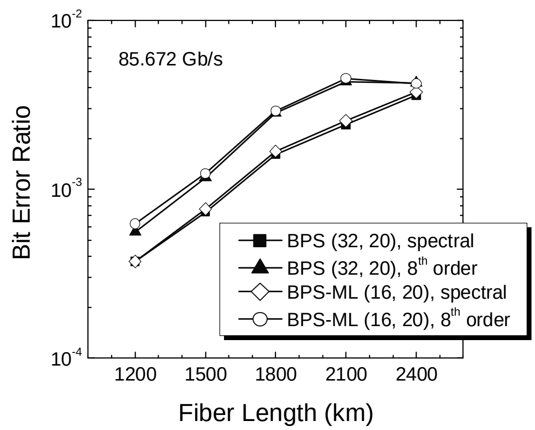

Figure 9. Dependence of the BER on fiber length for different combinations of frequency offset estimation algorithms and carrier phase estimation algorithms. The number of test phase angles for the BPS and BPS-ML algorithms is 32 and 16, respectively. The number of distance metrics for consecutive symbols that are summed to reduce the impact of amplified spontaneous emission noise is 20. 11-tap adaptive equalizer.

Finally, Figure 10 shows the dependence of the BER on fiber length for the three carrier phase estimation algorithms: BPS, two stage BPS, and BPS-ML. The performance of the BPS algorithm depends on the number of angles tested in the search for the one that minimizes a distance metric. The performance and complexity increase with the number of test angles, but with a diminishing improvement in the performance. With appropriate values for the parameters of each of the three algorithms, the resultant system performance is very similar.

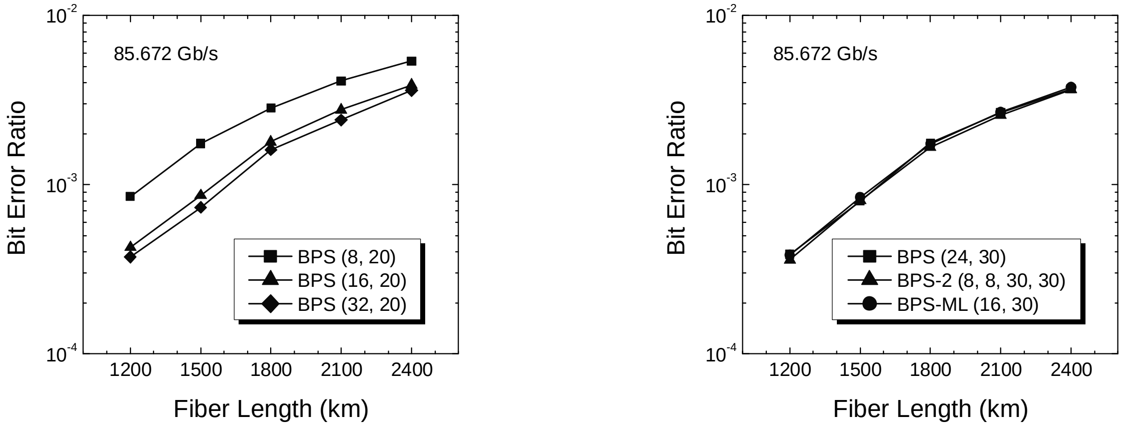

Figure 10. Left: dependence of the BER on fiber length for three values of the number of test phase angles in the BPS algorithm (8, 16, and 32). The number of distance metrics for consecutive symbols that are summed to reduce the impact of amplified spontaneous emission noise is 20. Right: dependence of the BER on fiber length for the BPS, two stage BPS (BPS-2), and BPS-ML algorithms. The number of test phase angles for the BPS, two stage BPS, and BPS-ML algorithms is 24, 8 (each stage) and 16, respectively. The number of terms that are summed to reduce the impact of amplified spontaneous emission noise is 30. 11-tap adaptive equalizer.

6. SUMMARY

The role of the signal processing algorithms on the transmission performance of coherent optical fiber communication systems has been considered for PM QPSK and PM 16-QAM signals. The algorithms typically have parameter values that must be set appropriately in order to obtain near-optimum performance and several examples have been used to illustrate this. The setting of these parameter values is generally not very strict. While different algorithms for the same function often yield similar performance, this is not ensured as dissimilar performance can be obtained.

REFERENCES

[1] K. Roberts, M. O'Sullivan, K.-T. Wu, H. Sun, A. Awadalla, D. J. Krause, and C. Laperle, “Performance of dual-polarization QPSK for optical transport systems,” J. Lightw. Technol. 27(16), 3546-3559 (2009).

[2] P. Winzer, A. H. Gnauck, C. R. Doerr, M. Magarini, and L. L. Buhl, “Spectrally efficient long-haul optical networking using 112-Gb/s polarization-multiplexed 16-QAM,” J. Lightw. Technol. 28(4), 547-556 (2010).

[3] S. Yamanaka, T. Kobayashi, A. Sano, H. Masuda, E. Yoshida, Y. Miyamoto, T. Nakagawa, M. Nagatani, and H. Nosaka, “11×171 Gb/s PDM 16-QAM transmission over 1440 km with a spectral efficiency of 6.4 b/s/Hz using high-speed DAC,” Proc. Eur. Conf. Opt. Commun., Torino, Italy, paper We.8.C.1 (2010).

[4] M. Nölle, J. Hilt, L. Molle, M. Seimetz, and R. Freund, “8×224 Gbit/s PDM 16QAM WDM transmission with real-time signal processing at the transmitter,” Proc. Eur. Conf. Opt. Commun., Torino, Italy, paper We.8.C.4 (2010).

[5] R. Schmogrow, D. Hillerkuss, M. Dreschmann, M. Huebner, M. Winter, J. Meyer, B. Nebendahl, C. Koos, J. Becker, W. Freude, and J. Leuthold, “Real-time software-defined multiformat transmitter generating 64QAM at 28 GBd,” IEEE Photon. Technol. Lett. 22(21), 1601-1603 (2010).

[6] B. Châtelain, D. Krause, K. Roberts, M. Chagnon, X. Xu, F. Gagnon, J. C. Cartledge, and D. V. Plant, “SPM-tolerant pulse shaping for 40 Gb/s and 100 Gb/s dual-polarization QPSK systems,” IEEE Photon. Technol. Lett. 22(22), 1641-1643 (2010).

[7] R. Schmogrow, M. Winter, M. Meyer, D. Hillerkuss, B. Nebendahl, J. Meyer, M. Dreschmann, M. Huebner, J. Becker, C. Koos, W. Freude, and J. Leuthold, “Real-time Nyquist pulse modulation transmitter generating rectangular shaped spectra of 112 Gbit/s 16QAM signals,” Proc. OSA Sig. Proc. Photon. Commun., paper SPMA4 (2011).

[8] T. Sugihara, T. Kobayashi, T, Fujimori, and T. Mizuochi, “Electronic pre-equalization technologies using high-speed DAC,” Proc. Eur. Conf. Opt. Commun., Geneva, Switzerland, paper Tu.6.B.2 (2011).

[9] S. Oda, T. Tanimura, Y. Cao, T. Hoshida, Y. Akiyama, H. Nakashima, C. Ohshima, K. Sone, Y. Aoki, M. Yan, Z. Tao, J. C. Rasmussen, Y. Yamamoto, and T. Sasaki, “80×224 Gb/s unrepeatered transmission over 240 km of large-A_{eff} pure silica core fibre without remote optical preamplifier,” Proc. Eur. Conf. Opt. Commun., Geneva, Switzerland, paper Th.13.C.7 (2011).

[10] J. C. Cartledge, J. D. Downie, J. Hurley, A. S. Karar, Y. Jiang, and K. Roberts, “Pulse Shaping for 112 Gbit/s Polarization Multiplexed 16-QAM Signals Using a 21 GSa/s DAC,” Proc. Eur. Conf. Opt. Commun., Geneva, Switzerland, paper We.7.A.5 (2011).

[11] K. Roberts, A. Borowiec, and C. Laperle, “Technologies for optical systems beyond 100G,” Opt. Fiber Technol. 17(5), 387-394 (2011).

[12] I. Fatadin, S. J. Savory, and D. Ives, “Compensation of quadrature imbalance in an optical QPSK coherent receiver,” IEEE Photon. Technol. Lett. 20(20), 1733-1735 (2008).

[13] H. Meyer, M. Moeneclaey, and S. A. Fechtel, Digital Communications Receivers, Wiley-Interscience, section 5.4 (1997).

[14] J. R. Treichler and B. G. Agee, “A new approach to multipath correction of constant modulus signals,” IEEE Trans. Acoust., Speech, Signal Processing ASSP-31(2), 459-472 (1983).

[15] S. J. Savory, “Digital filters for coherent receivers,” Opt. Exp. 16(2), 804-817 (2008).

[16] M. Morelli and U. Mengali, “Feedforward frequency estimation for PSK: a tutorial review,” Eur. Trans. Telecommun. 9(2), 103-116 (1998).

[17] Z. Tao, L. Li, A. Isomura, T. Hoshida, and J. C. Rasmussen, “Multiplier-free phase recovery for optical coherent receivers,” Proc. Conf. Optical Fiber Commun., paper OWT2 (2008).

[18] S. Zhang, P.Y. Kam, C. Yu, and J. Chen, “Decision-aided carrier phase estimation for coherent optical communications,” J. Lightw. Technol. 28(11), 1597-1607 (2010).

[19] M. G. Taylor, “Phase estimation methods for optical coherent detection using digital signal processing,” J. Lightw. Technol. 27(7) 901-914 (2009).

[20] I. Fatadin, D. Ives, and S. J. Savory, “Compensation of frequency offset for differentially encoded 16- and 64-QAM in the presence of laser phase noise,” IEEE Photon. Technol. 22(3), 176-178 (2010).

[21] J.-K. Hwang, Y.-L. Chiu, and C.-S. Liao, “Angle differential-QAM scheme for resolving phase ambiguity in continuous transmission system,” Int. J. Commun. Sys. 21(6), 631-641 (2008).

[22] M. Selmi, Y. Jaouën, and P. Cibalt, “Accurate digital frequency offset estimator for coherent polmux QAM transmission systems,” Proc. Eur. Conf. Opt. Commun., Vienna, Austria, paper P3.08 (2009).

[23] M. Li and L.-K. Chen, “Blind carrier frequency offset estimation based on eighth-order statistics for coherent optical QAM systems,” IEEE Photon. Technol. Lett. 23(21), 1612-1614 (2011).

[24] T. Pfau, S. Hoffmann, and R. Noé, “Hardware-efficient coherent digital receiver concept with feedforward carrier recovery for M-QAM constellations,” J. Lightw. Technol. 27(8), 989-999 (2009).

[25] J. Li, L. Li, Z. Tao, T. Hoshida, and J. C. Rasmussen, “Laser-linewidth-tolerant feedforward carrier phase estimator with reduced complexity for QAM,” J. Lightw. Technol. 29(16), 2358-2364 (2011).

[26] X. Zhou, “An improved feedforward carrier recovery algorithm for coherent receivers with M-QAM modulation format,” IEEE Photon. Technol. Lett. 22(14), 1051-1053 (2010).

[27] I. Fatadin, D. Ives, and S. J. Savory, “Blind equalization and carrier phase recovery in a 16-QAM optical coherent system,” J. Lightw. Technol. 27(15), 3042-3049 (2009).